

Supplementary Material for Strategies for the analysis of the elemental metal fraction of Ir and Ru oxides via XRD, XANES, and EXAFS

Anita Hamar Reksten* Frode Seland
Svein Sunde†

Department of Materials Science and Engineering, Norwegian University
of Science and Technology (NTNU) NO-7491 Trondheim, Norway

Andrea E. Russell and Peter W. Richardson
Stephen J. Thompson

Department of Chemistry, University of Southampton
Southampton SO17 1BJ, England

Karina Mathisen

Department of Chemistry, Norwegian University
of Science and Technology (NTNU), NO-7491 Trondheim, Norway

May 28, 2019

S.1 Effect of strain on Rietveld refinements

The Rietveld refinements may overestimate the metallic Ru fraction. For the ruthenium-rich samples, especially pure ruthenium, well described peak shapes in the refinements were not obtained. A super-Lorentzian contribution to the peaks was seen which could not be included in the fit. There

*Current address: SINTEF Sustainable Energy Technology, NO-0373 Oslo, Norway

†Corresponding author. Tel.: +47 73594051; fax: +47 73591105, *E-mail address*: Svein.Sunde@material.ntnu.no

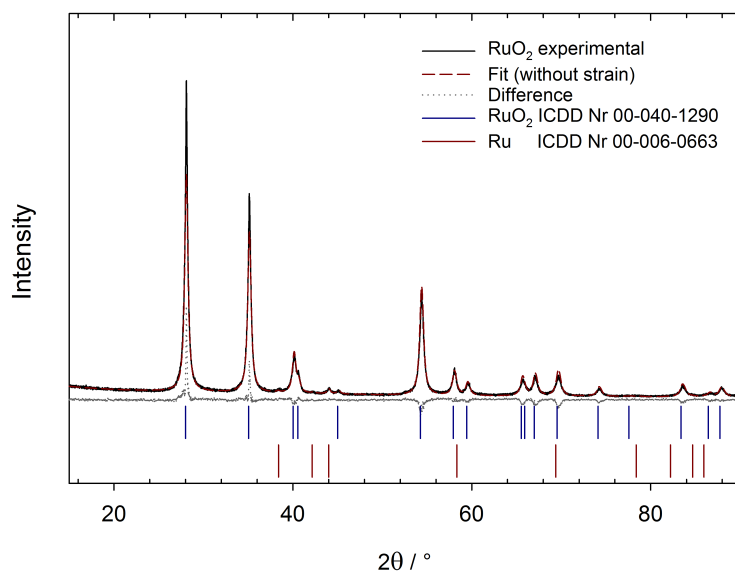
are several origins to peak broadening; any lattice imperfection will cause diffraction-line broadening, and domain-size broadening can occur if the powder consist of incoherent diffraction domains, such as dislocation arrays, stacking faults, twins or any other extended imperfections [1]. Investigation of the exact cause for the broadening seen in these samples was not performed. However, misfitting of the high intensity region of the peaks has consequences for the quantification. A strain parameter was added in order to include more of these areas. However, the omitted areas were small, and changes in fraction were insignificant (always < 0.4 wt.%) when strain was included in the fit. The contributions from the omitted high intensity peak region is therefore believed to be negligible in the phase quantification. The addition of the strain parameter did not effect the cell parameters. An example of refinement of $X_{\text{Ru}}=1$ is shown with and without strain added in Figure S.1. As can be seen the inclusion of strain improves the fit, however still a complete description of the most intense peaks is not obtained (Figure S.1b). Omitting the super-Lorentizian portion will also have consequences for the crystallite sizes obtained from the fit, and would be larger than indicated if these peak regions were well described. The sizes reported here are based on refinement carried out without added strain parameter, and can be looked upon as a lower limit of the crystallite size.

S.2 Microstructure

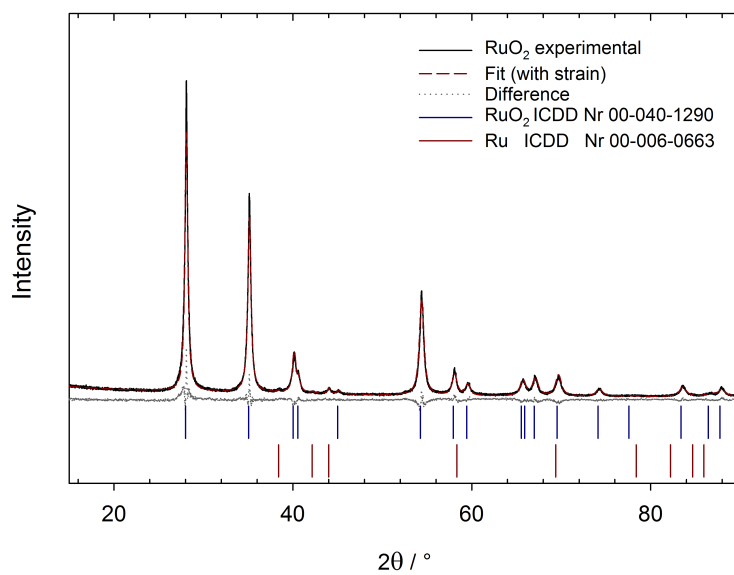
The morphology was investigated with SEM, and images of $X_{\text{Ru}}=0$, 0.5 and 1 are shown in Figure S.2. The samples contain large particles with diameter of several hundreds of nm, and smaller particles down to a few tenths of nm in diameter. The larger structures are in general larger for the Ru samples of both series, and smaller for Ir and the mixtures. The powders are in general agglomerated.

S.3 Crystallite size

In parallel to the increasing average particle diameter with ruthenium fraction, the crystallite sizes evaluated by Rietveld analysis were also found to increase with X_{Ru} , Figure S.3. Due to the broad structure and misfit of a super-Lorentzian part of the peaks (see ESI, Section S.1) of ruthenium-rich



(a) RuO₂ without strain parameter



(b) RuO₂ with strain parameter

Figure S.1: Rietveld refinement of XRD data for a RuO₂ sample refined without (a) and with (b) added strain parameter.

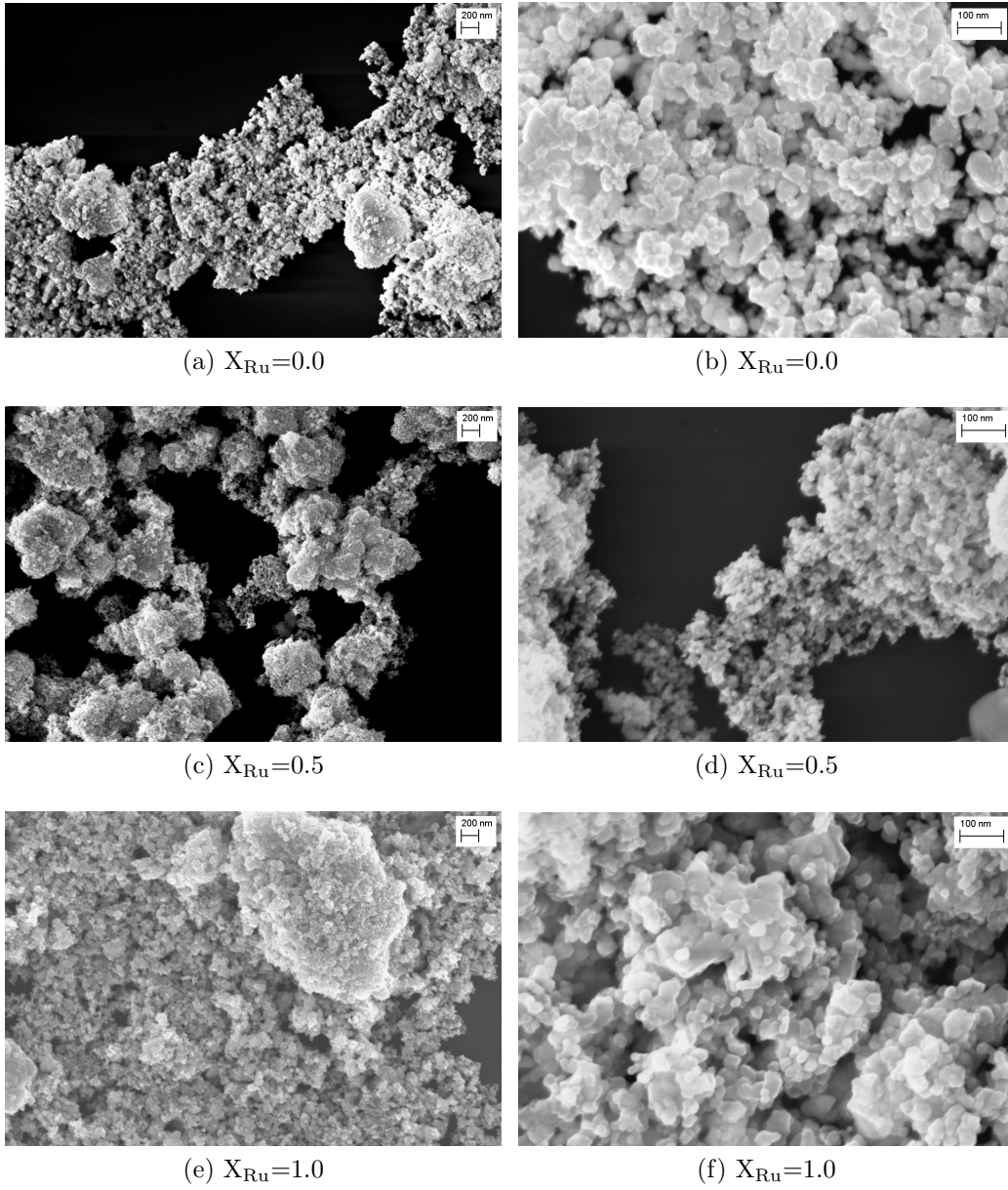


Figure S.2: SEM images of (a), (b) $X_{\text{Ru}}=0.0$, (c), (d) $X_{\text{Ru}}=0.5$ and (e), (f) $X_{\text{Ru}}=1.0$.

samples, the obtained and reported diameters can at best be looked upon as representing the smallest crystallites present. The diameters obtained increase with increasing ruthenium content. The increasing crystallite size with ruthenium fraction can be explained by lower crystallization temperature of ruthenium oxide and has been reported previously [2, 4].

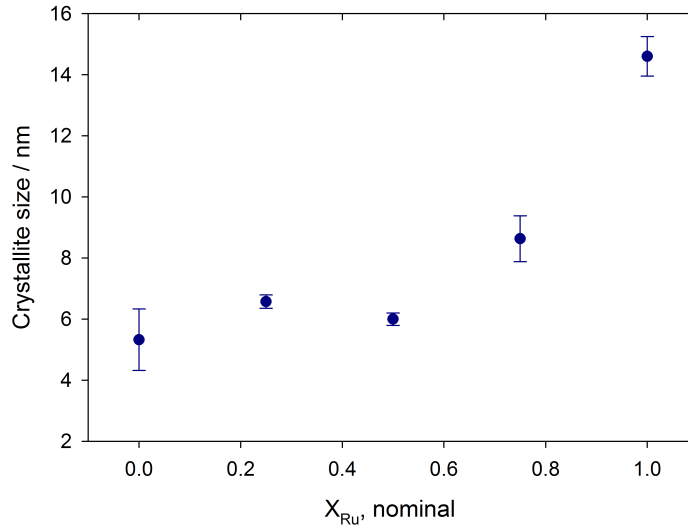


Figure S.3: Crystallite size of the oxide phase obtained by Rietveld refinement of X-ray diffractograms as a function of ruthenium fraction. Each data point is an average of the three samples of each composition, and the standard deviation of the three is indicated by error bars.

S.4 Conversion between atom percent and weight percent

The at.% iridium as obtained by linear-combination fitting of XANES is the number of iridium atoms in the metal reference sample Ir(0), n_{Ir} , divided by the total number of atoms in the two references Ir(0) and IrO₂ (n_{IrO_2}). Thus

$$\text{at.\%}(\text{Ir}) = 100 \times \frac{n_{\text{Ir}}}{n_{\text{Ir}} + n_{\text{IrO}_2}} \quad (\text{S.1})$$

The wt.% iridium metal as computed in the Rietveld analysis was [3, 5]

$$\text{wt.}\%(\text{Ir}) = 100S_{\text{Ir}}Z_{\text{Ir}}M_{\text{Ir}}V_{\text{Ir}} \times [S_{\text{Ir}}Z_{\text{Ir}}M_{\text{Ir}}V_{\text{Ir}} + S_{\text{Ir}_x\text{Ru}_{1-x}\text{O}_2}Z_{\text{Ir}_x\text{Ru}_{1-x}\text{O}_2}M_{\text{Ir}_x\text{Ru}_{1-x}\text{O}_2}V_{\text{Ir}_x\text{Ru}_{1-x}\text{O}_2} + S_{\text{Ru}}Z_{\text{Ru}}M_{\text{Ru}}V_{\text{Ru}}]^{-1} \quad (\text{S.2})$$

where Z_i is the number of formula units in the unit cell, S_i are scale factors adjusted during the refinement, M_i the molar mass, and V_i the unit cell volume in the phase of composition i . We use the convention here that $i = \text{Ir}$ refers elemental iridium (metal) and $i = \text{Ru}$ to elemental ruthenium. For ruthenium the wt.% metal was correspondingly

$$\text{wt.}\%(\text{Ru}) = 100S_{\text{Ru}}Z_{\text{Ru}}M_{\text{Ru}}V_{\text{Ru}} \times [S_{\text{Ir}}Z_{\text{Ir}}M_{\text{Ir}}V_{\text{Ir}} + S_{\text{Ir}_x\text{Ru}_{1-x}\text{O}_2}Z_{\text{Ir}_x\text{Ru}_{1-x}\text{O}_2}M_{\text{Ir}_x\text{Ru}_{1-x}\text{O}_2}V_{\text{Ir}_x\text{Ru}_{1-x}\text{O}_2} + S_{\text{Ru}}Z_{\text{Ru}}M_{\text{Ru}}V_{\text{Ru}}]^{-1} \quad (\text{S.3})$$

We let the scale factors correspond to the (relative) number of unit cells so that the number of iridium atoms n_{Ir} in the sample is proportional to $S_{\text{Ir}}Z_{\text{Ir}}$ etc. with the same proportionality factor for all phases. From (S.2) we obtain

$$\text{wt.}\%(\text{Ir}) = 100n_{\text{Ir}}M_{\text{Ir}} \times [n_{\text{Ir}}M_{\text{Ir}} + n_{\text{Ir}_x\text{Ru}_{1-x}\text{O}_2}M_{\text{Ir}_x\text{Ru}_{1-x}\text{O}_2}V_{\text{Ir}_x\text{Ru}_{1-x}\text{O}_2}/V_{\text{Ir}} + n_{\text{Ru}}M_{\text{Ru}}V_{\text{Ru}}/V_{\text{Ir}}]^{-1} \quad (\text{S.4})$$

where $n_{\text{Ir}_x\text{Ru}_{1-x}\text{O}_2}$ is the number of formula units of $\text{Ir}_x\text{Ru}_{1-x}\text{O}_2$ and $M_{\text{Ir}_x\text{Ru}_{1-x}\text{O}_2}$ its molar weight. Since the number of iridium atoms in the oxide phase, $n_{\text{Ir},\text{Ox}}$, is $n_{\text{Ir},\text{Ox}} = xn_{\text{Ir}_x\text{Ru}_{1-x}\text{O}_2}$, we may write Eq. (S.4) as

$$\text{wt.}\% = 100n_{\text{Ir}}M_{\text{Ir}} [n_{\text{Ir}}M_{\text{Ir}} + \frac{n_{\text{Ir},\text{Ox}}}{x}M_{\text{Ir}_x\text{Ru}_{1-x}\text{O}_2}V_{\text{Ir}_x\text{Ru}_{1-x}\text{O}_2}/V_{\text{Ir}} + n_{\text{Ru}}M_{\text{Ru}}V_{\text{Ru}}/V_{\text{Ir}}]^{-1} \quad (\text{S.5})$$

We divide numerator and denominator with $n_{\text{Ir}} + n_{\text{Ir},\text{Ox}}$ and use Eq. (S.1) to obtain

$$\begin{aligned} \text{wt.}\%(\text{Ir}) &= 100 [\text{at.}\%(\text{Ir})/100] M_{\text{Ir}} \\ &\times \left\{ [\text{at.}\%(\text{Ir})/100] M_{\text{Ir}} + \frac{1 - \text{at.}\%(\text{Ir})/100}{x} M_{\text{Ir}_x\text{Ru}_{1-x}\text{O}_2} V_{\text{Ir}_x\text{Ru}_{1-x}\text{O}_2}/V_{\text{Ir}} \right. \\ &\quad \left. + \frac{n_{\text{Ru}}}{n_{\text{Ir}} + n_{\text{Ir},\text{Ox}}} M_{\text{Ru}} V_{\text{Ru}}/V_{\text{Ir}} \right\}^{-1} \quad (\text{S.6}) \end{aligned}$$

For the samples with $X_{\text{Ru}} = 0$, the last term in the denominator of Eq. (S.4) is zero. For the samples with $X_{\text{Ru}} = 0.25$ we observe that dividing Eq. (S.2) by Eq. (S.3) gives

$$\frac{\text{wt.}\%(\text{Ir})}{\text{wt.}\%(\text{Ru})} = \frac{S_{\text{Ir}}Z_{\text{Ir}}M_{\text{Ir}}V_{\text{Ir}}}{S_{\text{Ru}}Z_{\text{Ru}}M_{\text{Ir}}V_{\text{Ru}}} = \frac{n_{\text{Ir}}M_{\text{Ir}}V_{\text{Ir}}}{n_{\text{Ru}}M_{\text{Ru}}V_{\text{Ru}}} \quad (\text{S.7})$$

Using this result in Eq. (S.6) we obtain

$$\begin{aligned} \text{wt.}\%(\text{Ir}) = & 100 \times [\text{at.}\%(\text{Ir})/100] M_{\text{Ir}} \times \\ & \left\{ [\text{at.}\%(\text{Ir})/100] M_{\text{Ir}} + \frac{1 - \text{at.}\%/100}{x} M_{\text{Ir}_x\text{Ru}_{1-x}\text{O}_2} V_{\text{Ir}_x\text{Ru}_{1-x}\text{O}_2} / V_{\text{Ir}} \right. \\ & \left. + \frac{1}{\text{wt.}\%(\text{Ru}) M_{\text{Ru}} V_{\text{Ru}} / \text{wt.}\%(\text{Ru}) M_{\text{Ir}} V_{\text{Ir}} + n_{\text{Ir},\text{Ox}} / n_{\text{Ru}}} M_{\text{Ru}} V_{\text{Ru}} / V_{\text{Ir}} \right\}^{-1} \quad (\text{S.8}) \end{aligned}$$

Since $\text{wt.}\%(\text{Ir}) \sim 40\%$ and $\text{wt.}\%(\text{Ru}) \sim 3\%$ in this sample,

$$\begin{aligned} & \frac{1}{\text{wt.}\%(\text{Ir}) M_{\text{Ru}} V_{\text{Ru}} / \text{wt.}\%(\text{Ru}) M_{\text{Ir}} V_{\text{Ir}} + n_{\text{Ir},\text{Ox}} / n_{\text{Ru}}} \\ & < \frac{1}{\text{wt.}\%(\text{Ir}) M_{\text{Ru}} V_{\text{Ru}} / \text{wt.}\%(\text{Ru}) M_{\text{Ir}} V_{\text{Ir}}} \approx 0.1 \end{aligned}$$

The factors multiplying the molar masses in the first two terms of the denominator of Eq. (S.7) are expected to be in the order of 0.5 and 2, respectively, which can be checked for consistency (see below). Also, the molar mass of ruthenium is approximately half of that of iridium. Whereas this is offset slightly by the volume ratios ($V_{\text{Ru}} = 81 \text{ \AA}^3$, $V_{\text{Ir}} = 56.6 \text{ \AA}^3$, $V_{\text{IrO}_2} = 63.3 \text{ \AA}^3$, $V_{\text{RuO}_2} = 63.3 \text{ \AA}^3$ for the conventional unit cells), the last term in the denominator of Eq. (S.4) is to a good approximation negligible. Therefore,

$$\text{wt.}\%(\text{Ir}) \approx \frac{100 \times [\text{at.}\%(\text{Ir})/100] M_{\text{Ir}}}{[\text{at.}\%(\text{Ir})/100] M_{\text{Ir}} + \frac{1 - \text{at.}\%/100}{x} M_{\text{Ir}_x\text{Ru}_{1-x}\text{O}_2}} \quad (\text{S.9})$$

in which we have also neglected the volume ratios being different from one, and from which we in turn obtain,

$$\begin{aligned} \text{at.}\%(\text{Ir}) \approx & \\ & 100 \times \frac{[\text{wt.}\%(\text{Ir})/100] M_{\text{Ir}_x\text{Ru}_x\text{O}_2} / x}{M_{\text{Ir}} (1 - \text{wt.}\%(\text{Ir})/100) + [\text{wt.}\%(\text{Ir})/100] M_{\text{Ir}_x\text{Ru}_{1-x}\text{O}_2} / x} \quad (\text{S.10}) \end{aligned}$$

For ruthenium the equations become

$$\text{wt.}\%(\text{Ru}) \approx 100 \times \frac{[\text{at.}\%(\text{Ru})/100] M_{\text{Ru}}}{[\text{at.}\%(\text{Ru})/100] M_{\text{Ru}} + \frac{1 - \text{at.}\%(\text{Ru})/100}{1 - x} M_{\text{Ir}_x\text{Ru}_{1-x}\text{O}_2}} \quad (\text{S.11})$$

$$\text{at.}\%(\text{Ru}) \approx 100 \times \frac{[\text{wt.}\%(\text{Ru})/100] M_{\text{Ir}_x\text{Ru}_{1-x}\text{O}_2} / (1 - x)}{M_{\text{Ru}} [1 - \text{wt.}\%(\text{Ru})/100] + [\text{wt.}\%(\text{Ru})/100] M_{\text{Ir}_x\text{Ru}_{1-x}\text{O}_2} / (1 - x)} \quad (\text{S.12})$$

for samples with no iridium metal in them.

X_{Ru} (nominal)	wt. Ir%	at.% Ir	wt. Ru%	at.% Ru	Sample
0	55.9	59.7			Table 1, sample 1
0	75.6	78.3			Table 1, sample 2
0	58.1	61.8			Table 1, sample 3
0.25	42.3	50.6			Table 1, sample 1
0.25	45.1	53.4			Table 1, sample 2
0.25	30.9	38.5			Table 1, sample 3
0	73.8	76.7			Table 4
0	67.7	71			Table 5
0.25	34.1	42			Table 4
0.75			14.3	25.5	Table 1, sample 2

Table S.1: Conversion of wt.% to at.% for various samples described in the main article as computed by Eqs. (S.9) through (S.12). Numbers in bold are the experimental values from which the other values are calculated.

References

- [1] D. Balzar. *J. Research of the National Institute of Standards and Technology*, 98:321–353, 1993.
- [2] J. Cheng, H. Zhang, G. Chen, and Y. Zhang. *Electrochimica Acta*, 54(26):6250 – 6256, 2009.

- [3] RJ Hill and CJ Howard. Quantitative Phase-Analysis From Neutron Powder Diffraction Data Using the Rietveld Method. *Journal of Applied Crystallography*, 20(6):467–474, DEC 1 1987.
- [4] A. Marshall, B. Børresen, G. Hagen, M. Tsyarkin, and R. Tunold. *Energy*, 32(4):431 – 436, 2007.
- [5] JC Taylor and CE Matulis. Absorption Contrast Effects in the Quantitative XRD Analysis of Powders by Full Multiphase Profile Refinement. *Journal of Applied Crystallography*, 24(1):14–17, FEB 1 1991.